



STRUCTURAL
BIOLOGY

Volume 77 (2021)

Supporting information for article:

Structural and thermodynamic insights into a novel Mg²⁺-citrate-binding protein of ABC transporter

Suraj Kumar Mandal and Shankar Prasad Kanaujia

Table S1 List of oligonucleotide sequences used for *mctA* and *mctA_mutant* recombinant constructs.

In *mctA_WT* construct, restriction enzyme recognition site and codon encoding the 6xHis-tag are underlined and shown in bold, respectively. Similarly, in mutant constructs, codons encoding a substituted amino acid are highlighted in bold and are underlined.

Primer	Oligonucleotide sequence (5'-3')
<i>mctA_WT_F</i>	ATAT <u>CATATGATGCAGCAGTC</u> CCGGCCTGCCTCGGAC
<i>mctA_WT_R</i>	ATAT <u>GGATCCTTA</u> ATGATGATGATGATG CTGGCCCCGGACGGC
<i>mctA_S26A_F</i>	CATCTACTCC <u>GCC</u> ACGGATCAATC
<i>mctA_S26A_R</i>	ATGAGGCGCCCTTCTTTC
<i>mctA_D28A_F</i>	TCCTCCAC <u>G</u> GCT CAATCCAGC
<i>mctA_D28A_R</i>	GTAGATGATGAGGCGCCC
<i>mctA_T55A_F</i>	TGATCTGGGT <u>GCC</u> CAAGCCAT
<i>mctA_T55A_R</i>	TTGTATTCAATCTGTATAAAGGGATAAAGTTG
<i>mctA_S79A_F</i>	TCTCTGGTCC <u>GCG</u> GCCATGGAGCTCCAGG
<i>mctA_S79A_R</i>	AGGTCTGCGCTGGAGGCT
<i>mctA_S164A_F</i>	CCCCGAGCGGG <u>GCC</u> GCCGTGGGC
<i>mctA_S164A_R</i>	TCCCAGGTGGCCACCCGC
<i>mctA_T199A_F</i>	CTACTCCTCC <u>GCC</u> GGGGCCGC
<i>mctA_T199A_R</i>	AGGGCGGCCTGGGCTTTG
<i>mctA_Y221A_F</i>	CTTCGGCTCC <u>GCG</u> GCCCTCCTCCGG
<i>mctA_Y221A_R</i>	AAGCCGTAGGCCAGGTAG
<i>mctA_Y221F_F</i>	TTCGGCTCC <u>TT</u> C GCCCTCCTC
<i>mctA_Y221F_R</i>	GAAGCCGTAGGCCAGGTAG
<i>mctA_R246A_F</i>	GGCCATCCAG <u>GCG</u> GTGGCCTTCATCAACAAG
<i>mctA_R246A_R</i>	ACGGTGCCGTGGTGAGG

Table S2 Composition of the crystallization buffer in which crystals were obtained for the wild type and mutant proteins of MctA along with its closest homolog Atu2467 (PDB id: 3C9H) for comparison.

S. No.	Protein	Crystallization buffer
1.	MctA_WT (FormI) (PDB id: 7F6E)	0.1 M sodium citrate tribasic dihydrate pH 5.5, 16% PEG 8000
2.	MctA_WT (FormII) (PDB id: 7F6F)	0.2 M ammonium fluoride, 20% PEG 3350
3.	MctA_WT (EDTA-treated) (PDB id: 7F6K)	0.2 M ammonium sulphate, 0.1 M MES monohydrate pH 6.5, 30% (w/v) PEG monoethyl ether 5000
4.	TTHB177_S26A_Mg ²⁺ -citrate (PDB id: 7F6N)	0.2 M ammonium fluoride, 20% PEG 3350
5.	MctA_S26A_Mn ²⁺ -citrate (PDB id: 7F6O)	0.2 M ammonium fluoride, 20% PEG 3350
6.	MctA_D28A (PDB id: 7F6P)	0.2 M ammonium phosphate dibasic, 20% PEG 3350
7.	MctA_S79A (PDB id: 7F6Q)	0.2 M ammonium sulphate, 0.1 M MES monohydrate pH 6.5, 30% (w/v) PEG monomethyl ether 5000
8.	MctA_S164A (PDB id: 7F6R)	0.01 M Co(II)Cl ₂ hexahydrate, 0.1 M MES monohydrate pH 6.5, 1.8 M ammonium sulphate
9.	MctA_T199A (PDB id: 7F6S)	0.2 M ammonium tartarate dibasic pH 7.0, 20% PEG 3350
10.	MctA_Y221A (PDB id: 7F6U)	0.2 M ammonium sulphate, 0.1 M Sodium cacodylate trihydrate pH 6.5, 30% (w/v) PEG 8000
11.	MctA_Y221F (PDB id: 7F6T)	0.2 M ammonium phosphate dibasic, 20% PEG 3350

Table S3 List of bacterial genera having proteins homologous to MctA with their Gram's property.

Microorganism (Genus) name	Gram's property	Query coverage (%)	Sequence identity (%)
Homology search against non-redundant proteins			
<i>Thermus</i> spp.	Gram-negative	96-100	89-98
<i>Deinococcus</i> spp.		93	55-58
<i>Proteobacteria</i> spp.		98	49
<i>Deltaproteobacteria</i> spp.		99	48
<i>Massilia</i> spp.		92-98	47-49
<i>Azospirillum</i> spp.		99	47
<i>Rhizobiales</i> spp.		96	47
<i>Duganella</i> spp.		92-98	47
<i>Pseudoduganella</i> spp.		92	47
<i>Janthinobacterium</i> spp.		92-96	45-48
<i>Rugamonas</i>		96	45
Homology search against the protein data bank			
<i>Agrobacterium</i> spp.	Gram-negative	89	37
<i>Actinobacillus</i> spp.		71	24

Table S4 Details of the proteins belonging to cluster D used for generating the structure-based distance tree for SBP classification.

Cluster	PDB id	UniProt id	Protein name	Organism name	Known ligand(s)
D	3K01	B0B0V1	GacH	<i>Streptomyces glaucescens</i>	Acarbose
	3UOR	Q8PK66	MalE	<i>Xanthomonas citri</i>	Maltose
	4MFI	A5U6I5	UgpB	<i>Mycobacterium tuberculosis</i>	Glycerophosphocholine

	3VXB	Q76BU9	BxIE	<i>Streptomyces thermophilus</i>	Xylooligosaccharide
	4H1X	P0C2M5	PstS2	<i>Streptococcus pneumoniae</i>	Phosphate
D-I	2B3B	Q72KX2	GGBP	<i>Thermus thermophilus</i>	Glucose
	3OO6	Q27GR2	AcbH	<i>Actinoplanes sp.</i>	Galactose
	3ZKK	A0A0J9X1B4	-	<i>Bifidobacterium animalis</i>	Sugar
	4G68	J9PBT4	-	<i>Caldanaerobius</i>	-
	4R2B	A6X5L9	-	<i>Ochrobactrum anthropi</i>	Sugar
D-II	1A99	P31133	PotF	<i>Escherichia coli</i>	Putrescine
	1POT	P0AFK9	PotD	<i>Escherichia coli</i>	Spermidine, Putrescine
	3RPW	Q6N0W2	-	<i>Rhodopseudomonas palustris</i>	-
	3TTM	Q9I6J1	SpuD	<i>Pseudomonas aeruginosa</i>	Putrescine
	4GL0	Q8Y8T4	-	<i>Listeria monocytogenes</i>	Spermidine, Putrescine
D-III-a	1ATG	Q7SIH2	ModA	<i>Azotobacter vinelandii</i>	Tungstate (VI)
	1WOD	P37329	ModA	<i>Escherichia coli</i>	Molybdate
	2H5Y	Q8PHA1	ModA	<i>Xanthomonas axonopodis</i>	Molybdate
	3CVG	J3KFC8	-	<i>Coccidioides immitis</i>	Metal
	3LR1	Q749P2	TupA	<i>Geobacter sulfurreducens</i>	Tungstate
	4RXL	Q9KLL7	-	<i>Vibrio cholerae</i>	Molybdate
D-III-b	2ONR	O30142	WtpA/Mo dA	<i>Archaeoglobus fulgidus</i>	Molybdate/ Tungstate

	3CFX	Q8TTZ5	ModA	<i>Methanosa</i> <i>acetivorans</i>	Tungstate
	3CFZ	Q58586	WtpA	<i>Methanocaldococcus</i> <i>jannaschii</i>	Molybdate/ Tungstate
	3CG1	Q8U4K5	WtpA	<i>Pyrococcus furiosus</i>	Molybdate/ Tungstate
	3CG3	O57890	WtpA	<i>Pyrococcus horikoshii</i>	Molybdate/ Tungstate
D-IV-a	1MRP	P35755	FbpA	<i>Haemophilus</i> <i>influenzae</i>	Iron
	1SI0	Q9Z4N6	FbpA	<i>Mannheimia</i> <i>haemolytica</i>	Iron
	1XVX	A1JLH5	YfuA	<i>Yersinia enterocolitica</i>	Iron
	1Y4T	Q0PBW4	CfbpA	<i>Campylobacter jejuni</i>	Iron
	2PT2	P72827	FutA1	<i>Synechocystis</i> sp.	Iron
D-IV-b	3C9H	Q7CWZ6	Atu2467	<i>Agrobacterium fabrum</i>	Mg ²⁺ -citrate

Table S5 Secondary structural content of MctA and its mutant proteins as determined using circular dichroism (CD) spectral analysis.

Protein	α-helix content (31.58)* (%)	β-sheet content (19.30)* (%)	Turns and others (49.12)* (%)
MctA_WT	34.5	16.1	49.4
MctA_S26A	38.9	14.4	46.7
MctA_D28A	34.2	16.8	49.0

MctA_T55A	22.0	24.8	53.2
MctA_S79A	37.4	15.1	47.5
MctA_S164A	35.1	13.9	51.0
MctA_T199A	36.2	15.4	48.4
MctA_Y221A	36.0	15.5	48.5
MctA_Y221F	40.0	15.0	45.0
MctA_R246A	22.0	24.8	53.2

* The secondary structural content (α helix, β -sheet, turns and others) based on the three-dimensional structure of MctA_WT are mentioned in the parenthesis.

Table S6 Thermodynamic parameters of various divalent metal ions binding to the mutant proteins MctA_S26A, MctA_S79A, and MctA_S164A where n, K_a , and K_d represent stoichiometry ratio, association constant, and dissociation constant, respectively.

Mutant proteins	Ligand	n	$K_a \times 10^6$ (M ⁻¹)	K_d (μM)	ΔH	$T\Delta S$	ΔG
					kcal mol ⁻¹		
MctA_S26A	MnSO ₄	1.13 ± 0.00	9.11 ± 2.23	0.11	-134.00	-124.56	-9.44

	CdCl ₂						
	MgCl ₂						
	NiCl ₂						
	CoCl ₂					No Binding	
	ZnCl ₂						
	FeSO ₄						
	Na-citrate						
MctA_S79 A	MnSO ₄	1.21 ± 0.01	1.12 ± 0.33	0.89	-11.74	-3.28	-8.46
	CdCl ₂	1.56 ± 0.01	0.04 ± 0.01	25.00	Data are beyond calorimetric determination		
	MgCl ₂	1.41 ± 0.01	0.12 ± 0.65	8.33			
	NiCl ₂	0.90 ± 0.02	0.03 ± 0.01	33.33			
	CoCl ₂	1.58 ± 0.02	0.02 ± 0.03	50.00			
	ZnCl ₂	1.49 ± 0.02	0.03 ± 0.01	33.33			
	FeSO ₄	No Binding					
	Na-citrate						
MctA_S164 A	MnSO ₄	0.91 ± 0.00	1.59 ± 0.23	0.63	-58.50	-48.60	-9.90
	CdCl ₂	1.27 ± 0.01	0.54 ± 0.27	1.85	-78.93	-70.62	-8.31
	MgCl ₂	0.99 ± 0.01	0.28 ± 0.12	3.60	-11.05	-3.28	-7.77

	NiCl_2	1.47 ± 0.01	0.68 ± 0.85	1.47	-71.39	-63.47	-7.92
	CoCl_2	1.13 ± 0.02	0.20 ± 0.16	5.00	-57.87	-50.06	-7.81
	ZnCl_2	1.77 ± 0.02	0.14 ± 0.30	7.14	-44.93	-36.65	-8.28
	FeSO_4	No Binding					
	Na-citrate						

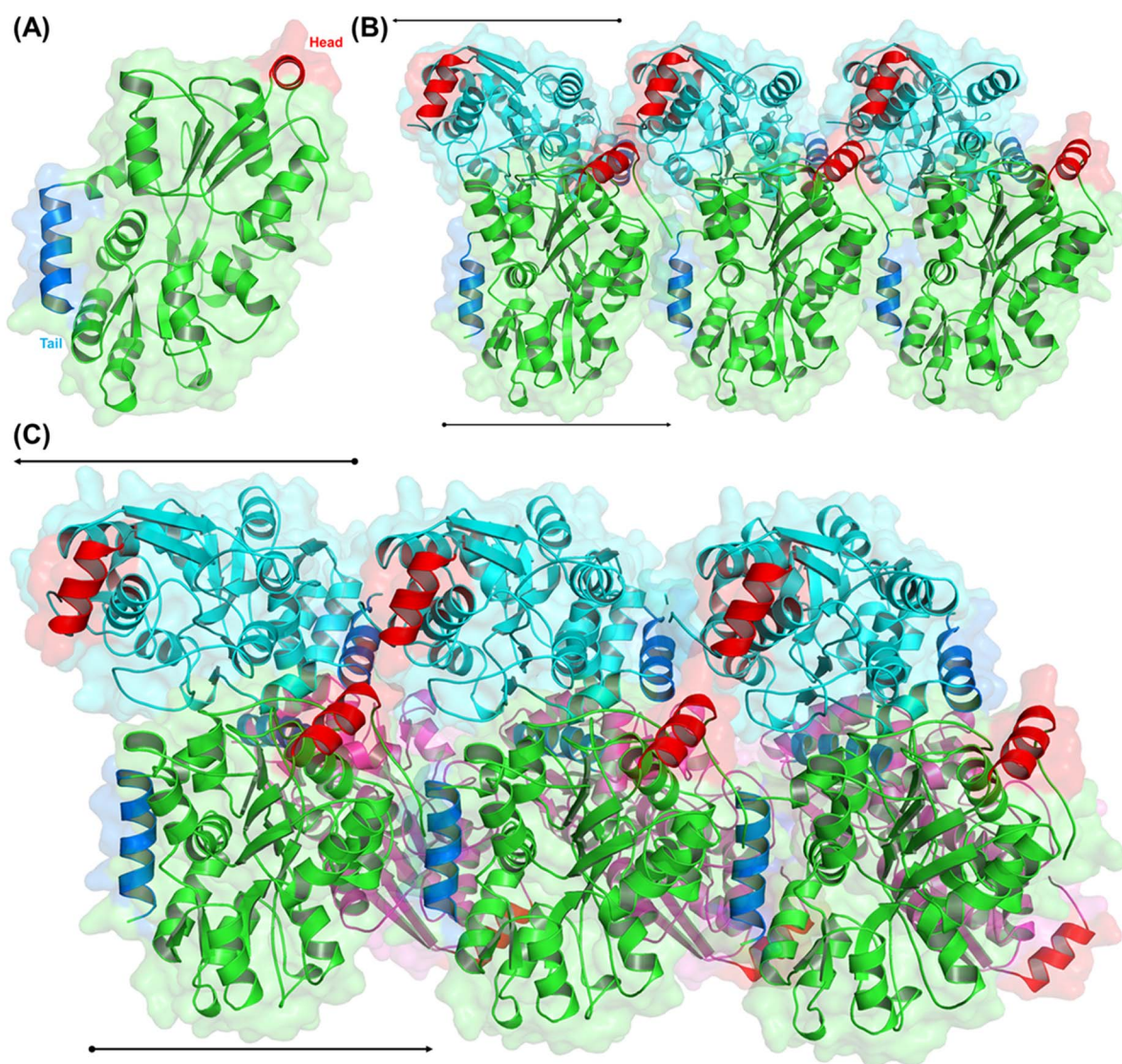


Figure S1 Arrangement of protein molecules in an asymmetric unit. (A) One protomer of MctA is represented in green. To get a clear view of protomer arrangement, its head and tail are demarcated in red and blue, respectively. (B and C) Protomer arrangement in the of MctA_FormII (space group: $P2_12_12_1$) and MctA_FormI (space group: $P2_1$). The three protomers of the asymmetric unit are colored in green, cyan, and magenta, respectively. The packing direction of protomers is represented with an arrow.

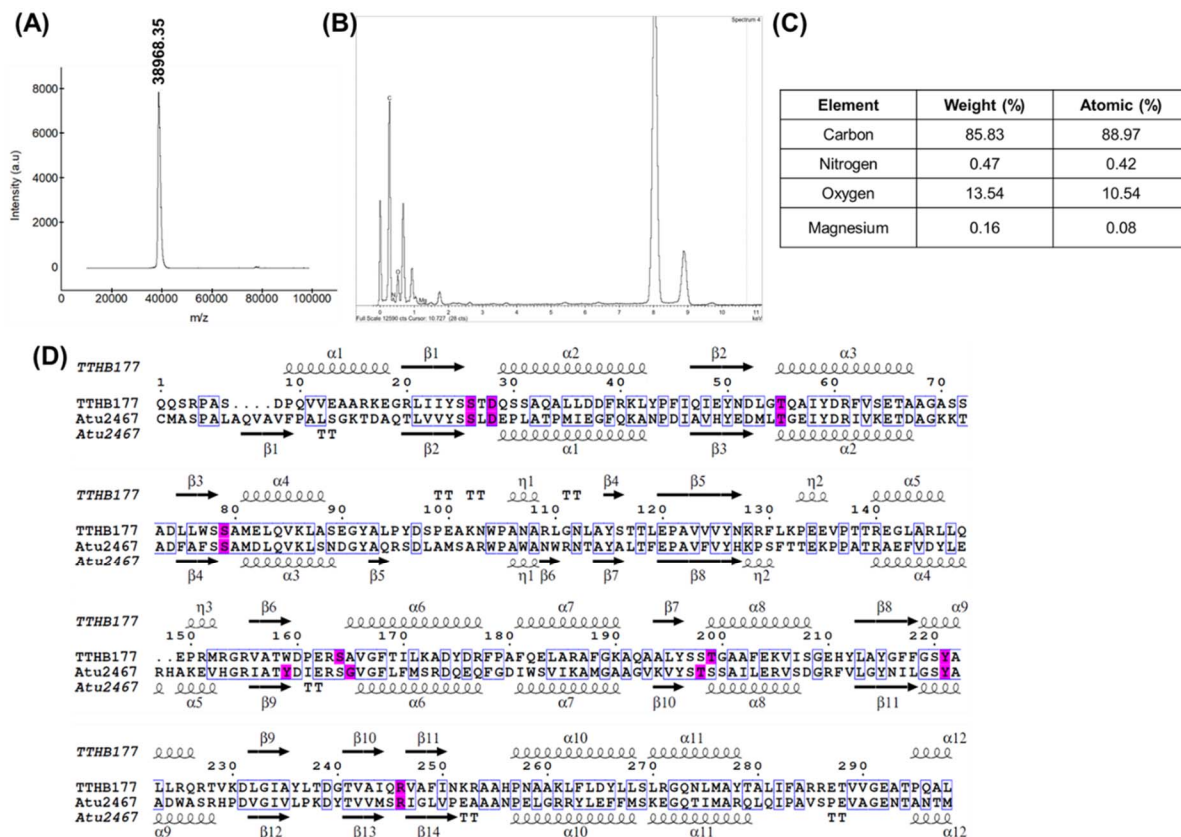


Figure S2 Mass spectrometric analysis and sequence comparison. (A) Mass spectrometric analysis of MctA_WT using MALDI-TOF. The obtained molecular weight of the protein in Daltons (unit) is labeled. (B) Energy dispersive X-ray (EDX) graph for MctA_WT. Y-axis represents the arbitrary intensity of elemental content. (C) The total elemental content of the protein solution is provided. (D) Secondary structure as well as sequence alignment of the proteins MctA with its closest homolog Atu2467. The residues interacting with the ligand molecule in both the proteins are highlighted in magenta. The secondary structural conservation is shown for MctA and Atu2467 in the top and bottom of the alignment, respectively.

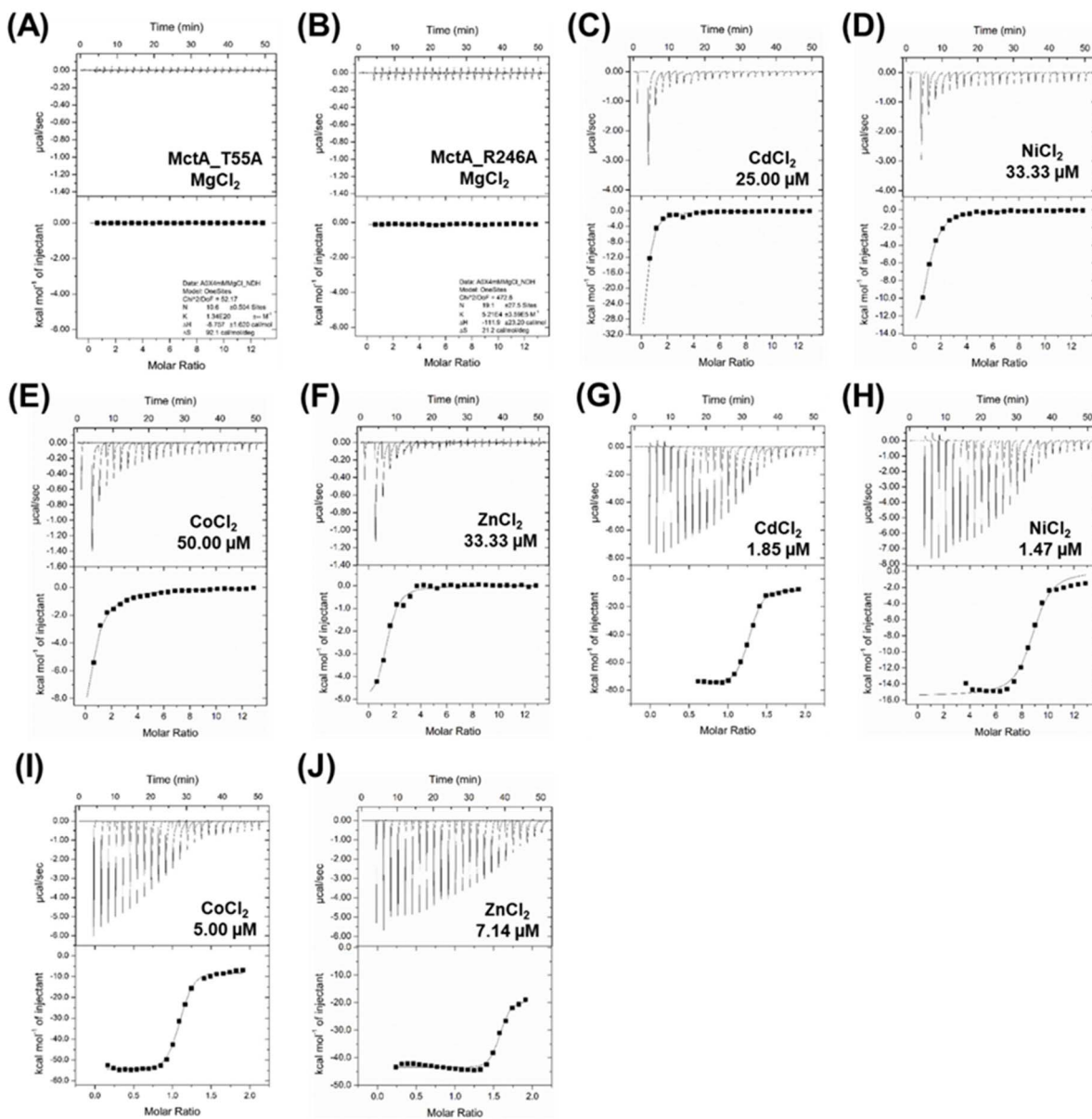


Figure S3 Thermodynamic data of the mutant proteins. Isothermal titration calorimetry of MctA_T55A and (B) MctA_R246A mutant showing their inability to bind MgCl_2 . ITC of MctA_S79A mutant with (C) CdCl_2 , (D) NiCl_2 , (E) CoCl_2 and (F) ZnCl_2 . ITC of MctA_S164A mutant with (G) CdCl_2 , (H) NiCl_2 , (I) CoCl_2 and (J) ZnCl_2 . (I)

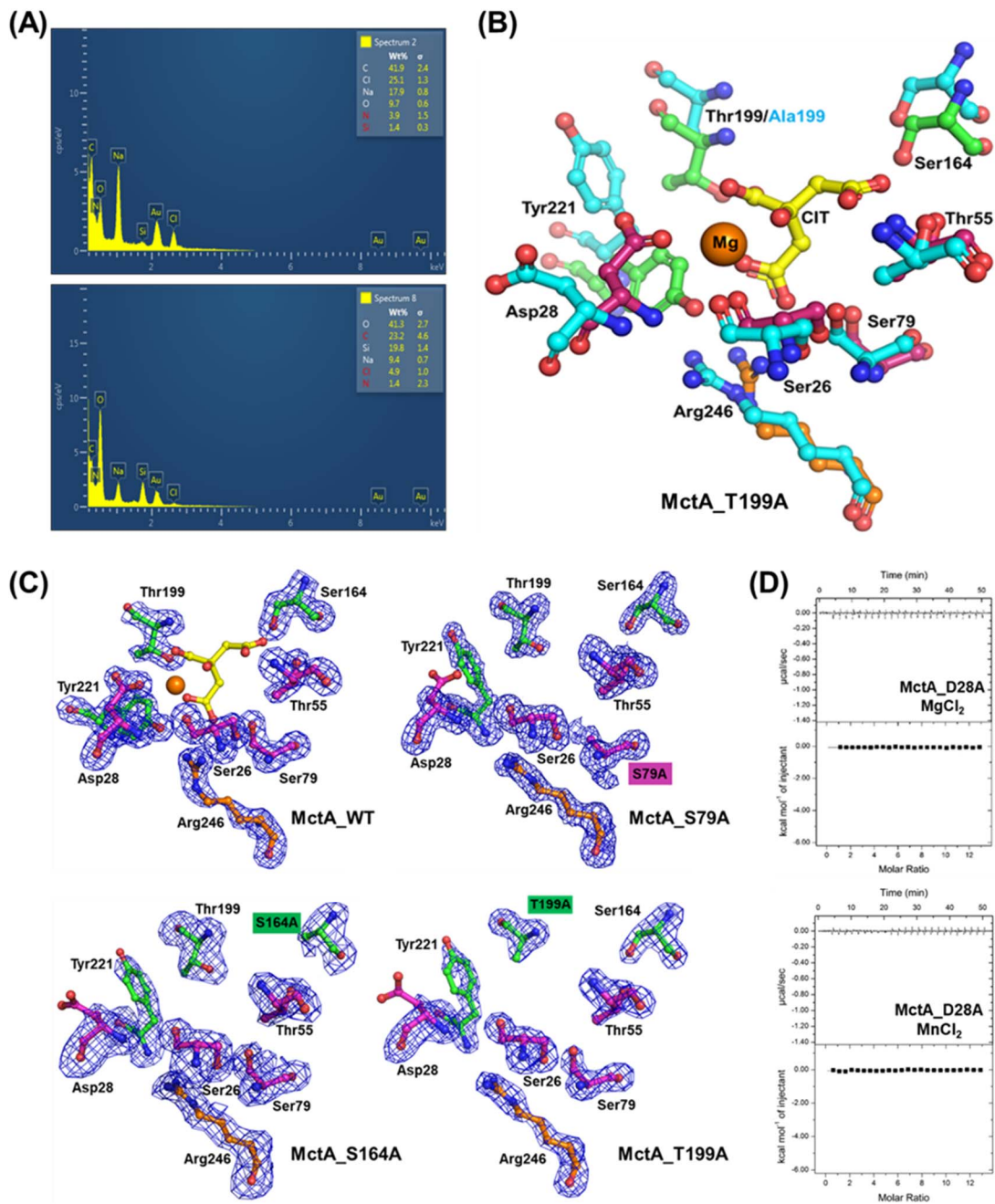


Figure S4 Mutational analysis of the protein MctA. (A) Energy dispersive X-ray (EDX) graph for the protein MctA_S79A (upper panel) and MctA_S164A (lower panel) showing the absence of Mg^{2+} ions in the solution. (B) Superposition of the active-site residues of the ligand-bound MctA_WT and ligand unbound MctA_T199A mutant. The active-site residues interacting in MctA_WT are represented as a cyan ball-and-stick model. (C) Comparison of the $F_o - F_c$ maps of the protein MctA_WT with MctA_S79A, MctA_S164A, and MctA_T199A mutants contoured at 3.0σ level. The interacting residues from the NTD, CTD, and hinge region are shown in warmpink, green, and orange, respectively. (D) ITC of the protein MctA_D28A showing its inability to bind $MgCl_2$ and $MnSO_4$.